

# CHARGE EXTRACTION ALONG THE IV CURVE OF A DYE-SENSITIZED NANOCRYSTALLINE SOLAR CELL: FURTHER INSIGHT INTO ELECTRON TRANSPORT, TRAPPING AND RECOMBINATION

Lobato K<sup>i</sup>, Peter LM<sup>ii</sup>

i) DEGGE, Sustainable Energy Systems of the University of Lisbon (SESUL) - klobato@fc.ul.pt  
ii) Dept. Chemistry, University of Bath - l.m.peter@bath.ac.uk

**ABSTRACT:** Charge transport within the oxide phase of a Dye-Sensitized Nanocrystalline Solar Cell is characterized and compared using two recently developed techniques; direct measurement of the internal quasi-Fermi level and charge extraction along the *iV* curve. The experimental results are compared to two models describing electron behaviour (diffusive electron transport and multiple trapping). The experimental results demonstrate good agreement with theory, and the two models are shown to be complimentary.

**Keywords** dye sensitized, characterisation, defects, defect density, experimental methods, fundamentals, modelling, TiO<sub>2</sub>, trapping, charge extraction, quasi Fermi level

## 1. INTRODUCTION

Dye-Sensitized Nanocrystalline Solar Cells (DSC) have great potential for being a viable method for electricity production. However, although the fabrication of the types of cells appears to be straight forward (and thus the potential for low costs), there is a great variety of factors that may influence the final performance and stability of these systems. This is due to the many components required to obtain a working cell (e.g.: transparent conductors, supporting oxides, light absorbing dyes, redox electrolytes, and counter-electrodes). Although this is a complex problem to solve it is nonetheless a challenge to bring together various different scientific areas and modifying one will have implications on others.

It is the balance of favourable energetics and kinetics of electron transfer between all the different components that give rise to the photovoltaic effect of these cells. Essentially the unfavourable kinetics are slower than the favourable kinetics (usually denoted as recombination) and thus electron transfer is directional to form a electric circuit.

One of the components of the cell that requires elucidation is the behaviour of electrons in the conducting oxide (usually TiO<sub>2</sub>). After the preparation of the oxide phase has been tuned for ease of deposition, or adsorbing of the active dye, there remains the important factor of how electrons behave within the TiO<sub>2</sub>; more specifically the electron diffusion length (diffusion coefficient and lifetime). Understanding this and how it may vary with different configurations or preparations of the cell is crucial in the optimisation of a complete cell.

The history of the understanding of electron transport in TiO<sub>2</sub> contacted by an electrolyte or in particle form is interesting to follow. Lindquist et. al.<sup>1</sup> showed that for compact TiO<sub>2</sub> films in contact with a hole capturing electrolyte, charge transport and collection was well described by charge separation being driving by an internal electric field at the semiconductor electrolyte interface. Unlike a conventional DSC, electron-hole pairs were created within the TiO<sub>2</sub>. Hagfeldt et. al.<sup>2</sup> performed a similar experiment except the compact layer was substituted by a porous layer (similar to that employed in DSCs). The results proved to be very different and were argued by the authors that because charge separation occurred homogenously, charge collection was not determined by the efficiency in which charge separation occurred, but by the distance the electrons had to travel to be collected before recombining. Sodergren et. al.<sup>3</sup> then showed the results of Hagfeldt et. al.<sup>2</sup> could be described if electron transport in the porous oxide were diffusive. In fact they went as far as deriving expressions describing the *iV* characteristic of a DSC.

TiO<sub>2</sub> particles are n-type with the Fermi level close or in to the conduction band. When the TiO<sub>2</sub> particle comes into contact with an electrolyte (typically I/I<sub>3</sub><sup>-</sup> redox couple where the redox potential is c.a. 1eV below the conduction band of TiO<sub>2</sub>), all electrons are extracted from the TiO<sub>2</sub> and thus becomes depleted of charge, hence insulating. However, because of the dimensions of the particles, there is an insignificant potential gradient and thus negligible electric fields.<sup>4</sup> This is why the driving force for electron transport within the oxide phase of a DSC has to be diffusion driven.

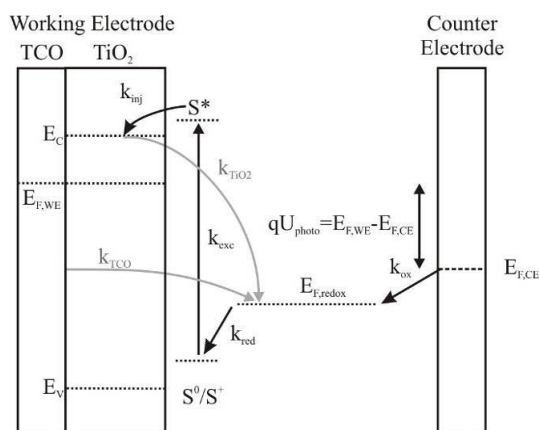


Figure 1 Schematic rendition of the DSC illustrating the competing mechanisms.  $k_{inj}$  - injection rate constant from dye to the oxide,  $k_{exc}$  - excitation rate constant from the HOMO to the LUMO,  $k_{TiO_2}$  - recombination rate constant from the oxide to the electrolyte,  $k_{TCO}$  - recombination rate constant of electrons from the TCO to the electrolyte,  $k_{red}$  - reduction rate constant of dye molecules by the electrolyte and  $k_{ox}$  - oxidation rate constant of the counter electrode with the electrolyte. Shown, too, are the relative positions of the energy levels of the conduction band  $E_C$ , valence band  $E_V$ , LUMO and HOMO levels, the electrolyte redox potential  $E_{F,redox}$ , along with the splitting of the quasi-Fermi level  $E_F$ , at the working and counter electrodes.

One may argue that some confusion or distraction occurred when dynamic measurements were used to characterise electron transport, demonstrating odd behaviours such as large electron densities<sup>5</sup> (far greater than what could be expected in the conduction band), slow response times<sup>6</sup> and highly variable diffusion and electron lifetimes<sup>7</sup> depending on bias potentials or illumination intensities.

In fact it appears that there is an inter-bandgap trap distribution which plays a crucial role when dynamic measurements are performed. Essentially they act as a buffer (due to their filling and emptying), and play a significant role because the occupation density of these by electrons is far greater than those occupying the conduction band.

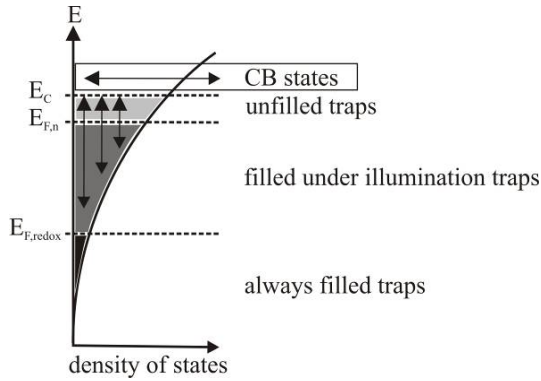


Figure 2 Schematic representation of the multi trapping mechanism with an exponential trap distribution. Traps below the redox potential are always filled. As the QFL is increased, traps below this energy will be filled, while those above it remain empty. However, there is an equilibrium of conduction band electrons constantly trapping, and trapped electrons detrapping. It is generally found for DSCs that the trap distribution follows an exponential profile, their density increasing as a function of energy.<sup>5</sup>

These effects on dynamic measurements were elegantly explained by Bisquert et. al.<sup>8</sup> employing the quasi-static approximation. It must be noted that it is the information acquired from steady-state measurements that is of interest to photovoltaic efficiency. However, dynamic measurements when correctly employed to account for the trap occupation and the real position of the quasi-Fermi level can be used to determine electron lifetimes and diffusion coefficients<sup>9</sup>. What occurs is that although the electron lifetime and diffusion coefficients vary considerably if measured using dynamic measurements, the diffusion length remains unchanged.

Jennings et. al.<sup>9</sup> in fact utilise the idea introduced by Bisquert et. al.<sup>8</sup> (apparent electron lifetimes and diffusion coefficients) along with the possibility of measuring the position of the QFL within the TiO<sub>2</sub><sup>10</sup> to show that the diffusion length of electrons in DSCs employing a solid hole conductor is greater than initially thought. The important point to note about the work presented by Jennings et. al.<sup>9</sup> is that it brings together two complementary models of diffusion driven electron transport<sup>3</sup> and the multiple trapping model<sup>8</sup>. Here a similar comparison is drawn between the two.

## 2. THEORY

It has previously been shown that it is possible to directly probe the position of the QFL within the oxide phase of the DSC when illuminated and under various different applied biases and conditions<sup>10, 11</sup>.

To start, the continuity equation is solved for steady state conditions;

$$0 = I_0 \alpha e^{-\alpha x} + D_0 \frac{\partial^2 n_C(x)}{\partial x^2} - \frac{n_C(x) - n_{eq}}{\tau_0} \quad (1)$$

Where:  $I_0$  is the incident photon flux;  $\alpha$  is the absorption coefficient;  $x$  is position within the TiO<sub>2</sub> film where  $x=0$  is the FTO|TiO<sub>2</sub> interface;  $D_0$  is the absorption coefficient,  $n_{C(x)}$  is the electron density;  $n_{eq}$  is the dark equilibrium electron density (determined by the difference of the redox potential energy and the conduction band edge); and  $\tau_0$  is the electron lifetime. The boundary conditions applied are, firstly the extraction at the FTO|TiO<sub>2</sub> interface is sufficiently rapid so that the electron density at this interface is defined by the applied external voltage, i.e.;

$$qU_{photo} = k_B T \ln \frac{n_C}{n_{eq}} \quad (2)$$

This boundary condition defines the electron flux at the interface (which translates to the current the cell generates);

$$j = -D_0 \left. \frac{dn}{dx} \right|_{x=0} \quad (3)$$

Secondly, the electron density profile at  $x=d$  is flat. Solving<sup>4</sup> for the electron density profiles the local QFL (which can be measurable) is defined by;

$$n_C(x) = N_C \exp\left(-\frac{E_C - E_F(x)}{k_B T}\right) \quad (4)$$

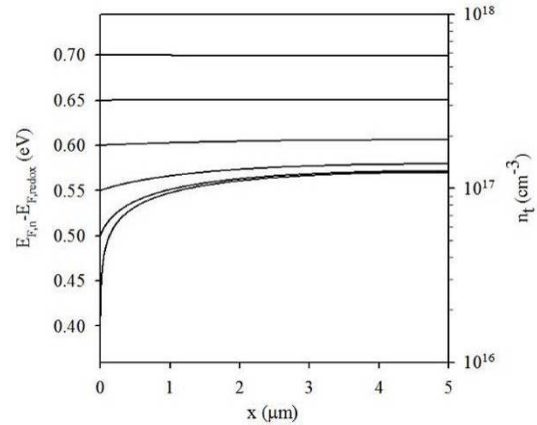


Figure 3 Example of how the QFL and the resultant trapped electron density varies for different biases at  $x=0$  under illumination (1 c.a. 1 sun). Physical parameters were:  $D_0=0.04\text{cm}^2\text{s}^{-1}$ ;  $\tau_0=1\text{ms}$ ;  $E_C-E_{F,redox}=0.95\text{eV}$ ,  $N_C=10^{21}\text{cm}^{-3}$ ,  $N_t=10^{19}\text{cm}^{-3}$ ,  $T_C=1000\text{K}$ . The density of trapped electrons is directly proportional to the QFL so only one set of curves is required to represent both. Electron flow will from right to left to the extracting electrode at  $x=0$ .

With the insertion of the sensing electrode it is possible to measure the QFL at  $x=d$ , where  $d$  is the thickness of the TiO<sub>2</sub> layer (usually 1 to 20 $\mu\text{m}$ ). It must be noted that under steady state conditions the trapping

effects are irrelevant because of the nature of the traps, these not being recombination centres and thus does not form part of the formulation to determine lifetime. Also transport is assumed to be the conduction band and not by some hopping mechanism from trap site to trap site.

Figure 3 illustrates some QFL profiles for various applied biases under illumination. To note is that even under short circuit conditions there is a significant QFL level within the film, c.a. 500mV and has been confirmed previously<sup>10</sup>.

Knowing the trap distribution it is straight forward to calculate the trap occupancy throughout the film. The local trapped electron density at  $x$  is determined by the local QFL level  $E_F(x)$ . For an exponential trap distribution the trapped electron density is given by;

$$n_t(x) = N_t \exp \frac{E_F(x) - E_C}{k_B T_C} \quad (5)$$

The trap density of a DSC tends to follow an exponential profile with a characteristic temperature  $T_C$  (or  $\beta = T/T_C$ ). With an electron density profile, and thus a QFL profile we now also have a trapped electron density profile. Integrating from  $x=0$  to  $x=d$  one has the total trapped electron density for different applied biases and under illumination (i.e. along the iV curve). It is this additional quantity which is measured and used to test the theory.

### 3. Results and Conclusions

To measure the trapped electron density along the iV curve it was necessary to modify the method used to characterise the trapped electron density<sup>5</sup>. Essentially the cell was held at a point along the iV curve and then short-circuited as the illumination was simultaneously cut-off. The result is that the QFL begins to drop as the electron detrap and are collected. It is this value which is integrated to measure the trapped electron density. More details on the specific requirements of the experimental setup are published elsewhere<sup>4</sup>.

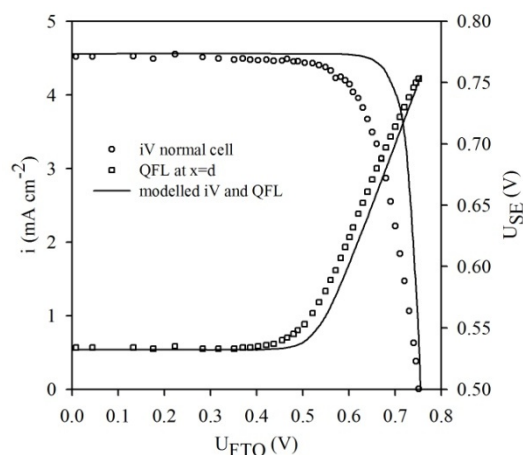


Figure 4 measured and calculated iV curve and the internal QFL.

The results in Figure 4 and Figure 5 illustrate that by calculating the QFL profile throughout the film one can then infer the trapped electron density. This integrated result confirms that although the QFL can only be probed at two points ( $x=0$  and  $x=d$ ) the QFL profiles are most

likely to be that calculated, because the trapped electron density follows the same tendencies as predicted for each QFL profile at different points along the iV curve. However agreement is not perfect under short circuit conditions. Reasons could be various such as imperfect characterisation of the trap distributions or abarations of the measured internal QFL by the introduction of the sensing electrode. Nonetheless this is further evidence that in principle electron transport is dominated by diffusion and that the trap states occur homogeneously throughout the film. This is also a further technique to narrow down the range of values the physical parameters can take. This is critical because there appears to be more variables than individual measurements to pin down the values of the individual physical parameters. A full analysis of the range of values these can take is currently being worked upon.

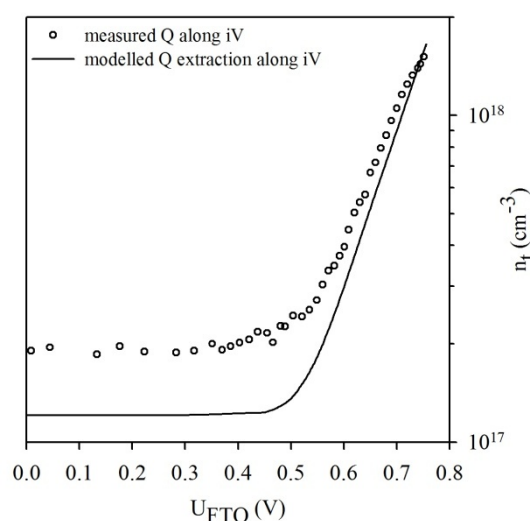


Figure 5 Measured and calculated trapped charge along the iV curve.

### 4. REFERENCES

- 1 Lindquist S. E., et al., *Journal of the Electrochemical Society*, 1983, vol.130(2), 351-358
- 2 Hagfeldt A., et al., *Solar Energy Materials and Solar Cells*, 1992, vol.27(4), 293-304
- 3 Sodergren S., et al., *Journal of Physical Chemistry*, 1994, vol.98(21), 5552-5556
- 4 Lobato K., *Charge transport and recombination in dye-sensitized nanocrystalline solar cells*, University of Bath, 2007
- 5 Bailes M., et al., *Journal of Physical Chemistry B*, 2005, vol.109(32), 15429-15435
- 6 Schwarzburg K., et al., *Applied Physics Letters*, 1991, vol.58(22), 2520-2522
- 7 Peter L. M., et al., *Electrochemistry Communications*, 1999, vol.1(12), 576-580
- 8 Bisquert J., et al., *Journal of Physical Chemistry B*, 2004, vol.108(7), 2313-2322
- 9 Jennings J. R., et al., *J. Phys. Chem. C*, 2007, vol.111(44), 16100-16104
- 10 Lobato K., et al., *Journal of Physical Chemistry B*, 2006, vol.110(33), 16201-16204
- 11 Lobato K., et al., *Journal of Physical Chemistry B*, 2006, vol.110(43), 21920-21923